Supporting Information

MOF-derived noble-metal-free Cu/CeO_2 with high porosity for efficient water–gas shift reaction at low temperatures

Deshetti Jampaiah,[a,b] Devaiah Damma,[c] Anastasios Chalkidis,[a] Mandeep Singh,[b] Ylias M. Sabri,[a] Edwin L. H. Mayes,[d] Vipul Bansal[b] and Suresh K. Bhargava*[a]

[a]Centre for Advanced Materials and Industrial Chemistry (CAMIC), School of Science, RMIT University, Melbourne VIC 3000, Australia.

[b]Ian Potter NanoBioSensing Facility, NanoBiotechnology Research Laboratory, School of Science, RMIT University, Melbourne VIC 3000, Australia.

[c]Chemical Engineering, College of Engineering and Applied Science, University of Cincinnati, Cincinnati, Ohio 45221−0012, United States of America

[d]RMIT Microscopy and Microanalysis Facility, School of Science, RMIT University, Melbourne VIC 3000, Australia

*Email: suresh.bhargava@rmit.edu.au

Experimental Details

Synthesis of Ce-BTC and CuCe-BTC templates

The synthesis of CeO_2-BTC (Ce-BTC) template was based on the following procedure: Firstly, 4.34 g of cerium (III) nitrate hexahydrate (10.0 mmol) and 1.40 g of trimesic acid (benzene-1,3,5-tricarboxylic acid) (6.67 mmol) were sealed into a 100 mL of Teflon-lined hydrothermal synthesis autoclave and heated to 100°C for 24 h with 60 mL of dimethylformamide (DMF). The resulting white crystalline powder was extracted and washed twice with hot ethanol to remove impurities and excess DMF and then dried in a vacuum oven at 100°C for 24 h. A similar approach was used to prepare CuCe-BTC template. For CuCe-BTC, the Cu/Ce ratio was 9/1. Briefly, 0.295 g of copper nitrate and 3.906 g of cerium nitrate precursors were mixed with 1.40 g of trimesic acid (6.67 mmol) and transferred to a 100 mL of Teflon-lined hydrothermal synthesis autoclave and heated to 100°C for 24 h with 60 mL of DMF.

Synthesis of nanoporous CeO_2 and Cu/CeO_2

The as-synthesized Ce-BTC was grounded into a powder and then heated at a rate of 5°C min–1 under an N_2 (g) stream with a flow rate of 100 mL min^{-1}. The material was maintained at the target temperature of 500°C for 6 h. After the sample had cooled down to room temperature, a second heat treatment was used to remove the organic species and activate the preformed pores. The material was heated with a rate of 1 °C min^{-1} in the presence of O_2 (g) and maintained at the target temperature of 400°C for 3 h. After the sample had cooled to room temperature, the desired solid was obtained. Similarly, the Cu/CeO_2 catalyst was obtained after calcination process as mentioned above. To investigate the importance of MOF template approach, similar catalysts were prepared by co-precipitation method. Briefly, 4.34

g of cerium nitrate precursor was dissolved in 100 mL of distilled water and added aqueous ammonia (25 wt.%) drop-wise. The solution gets precipitated once the pH reaches 9. After, the precipitate was washed several times with water and ethanol and obtained precipitated CeO_2 followed by drying and calcination at 400°C for 3 h. Similar procedure was followed for co-precipitated Cu/CeO_2 catalyst, in which 0.295 g of copper nitrate and 3.906 g of cerium nitrate were used as precursors. The loading of CuO was maintained at 10 wt.%.

Catalyst characterization

Microwave plasma atomic emission spectrometry (MP-AES; 4210, Agilent) was carried out to determine the bulk elemental composition of materials. Prior to this analysis, a certain amount of each powder was dissolved in nitric acid and was diluted with deionized water. Scanning electron microscopy (FEI Verios SEM operated at 15 kV) was used to determine the surface morphology of the samples. Transmission electron microscopic (TEM) images and selected area electron diffraction (SAED) patterns were recorded on a JEOL 1010 instrument operating at 100 kV. High-resolution transmission electron microscopy (HR–TEM) studies were carried out on a JEOL 2100F microscope with an operating voltage of 200 kV. Before TEM analysis, the samples were well dispersed in isopropanol by sonication and coated on a nickel grid. A powder X-ray diffraction (XRD; Bruker D8 Discover micro diffraction system) instrument equipped with a Cu Kα (1.51406 Å) radiation source was used to identify the crystalline phases of the samples. CuO crystallite size and Cu dispersion of the as-prepared catalysts were determined by N_2O chemisorption, which was conducted by AutoChem II 2920 instrument. Before N_2O chemisorption, the catalysts were reduced at 400°C for 1 h under H_2 environment. Then, the catalysts were exposed to 5 vol% N_2O with diluted He gas and the amount of Cu was measured by thermal conductivity detector (TCD). The amount of Cu was

determined by the following equations ($N_2O + 2Cu = Cu_2O + N_2$). Specific surface areas (S_{BET}) of the samples were obtained on a Micromeritics (ASAP 2400) analyser at liquid nitrogen (N_2) temperature (-196°C) using the Brunauer–Emmett–Teller (BET) method. Raman spectra of the samples were recorded on a Horiba LabRAM HR evolution Raman spectrometer using a 532 nm laser source. The surface elemental analysis was carried out by using X-ray photoelectron spectroscopy (XPS) (Thermo K-alpha) with an Al Kα (1486.7 eV) radiation source at room temperature under ultra-high vacuum (10^{-8} Pa). After the reduction treatment, the samples were exposed to the atmosphere prior to XPS analysis. The hydrogen temperature programmed reduction (H_2–TPR) of various catalysts was performed on a Micromeritics instrument (AutoChem II 2920) equipped with a TCD. For each TPR test, 50 mg of the sample was used with pre-treatment under a He atmosphere before the analysis. The sample was then heated up to 700 °C at 5 °C min^{-1} in a flow of 10% H_2/Ar (10 mL min^{-1}). Finally, the H_2 consumption was monitored using a TCD detector.

Catalytic activity measurements

The water-gas shift reaction (WGS) was conducted from 150 to 400°C under atmospheric pressure in a vertical down flow fixed-bed quartz reactor. The catalytic activity was performed using 50 mg of catalyst powder. Prior to the reaction, the catalyst was reduced at 400°C for 1 h under H_2 environment. The WGS reaction was carried out with a GHSV of 60,000 h^{-1}. The WGS reactants (CO and H_2O) were fed to the reactor at a steam to CO ratio of 3.5 with a total flow of 50 mL min^{-1}. Water was injected into a flowing gas stream by an ISCO series D pump controller and vaporized at 150°C using heating tape before entering the reactor. The outlet gas streams were passed through an ice-cooled trap to condense the unreacted water from the reaction and subsequently analysed by an online gas chromatograph equipped with a

Porapak Q column and TCD. The readings were collected when the reaction reached steady-state.

Kinetic analysis for WGS reaction

To obtain kinetics data, the experiments were conducted under differential reactor approach and mass transfer free operating conditions with CO conversion below 20% for the catalysts in the range of 180 to 340 °C. The catalytic activation energy (E_a) of the catalysts were calculated according to the Arrhenius equation (2).

$$R = Ae^{(-Ea/RT)} \qquad (2)$$

where E_a, apparent activation energy (kJ/mol); R, the reaction rate ($mol \cdot s^{-1} \cdot m^{-2}$); T, the value of the reaction temperature (K).

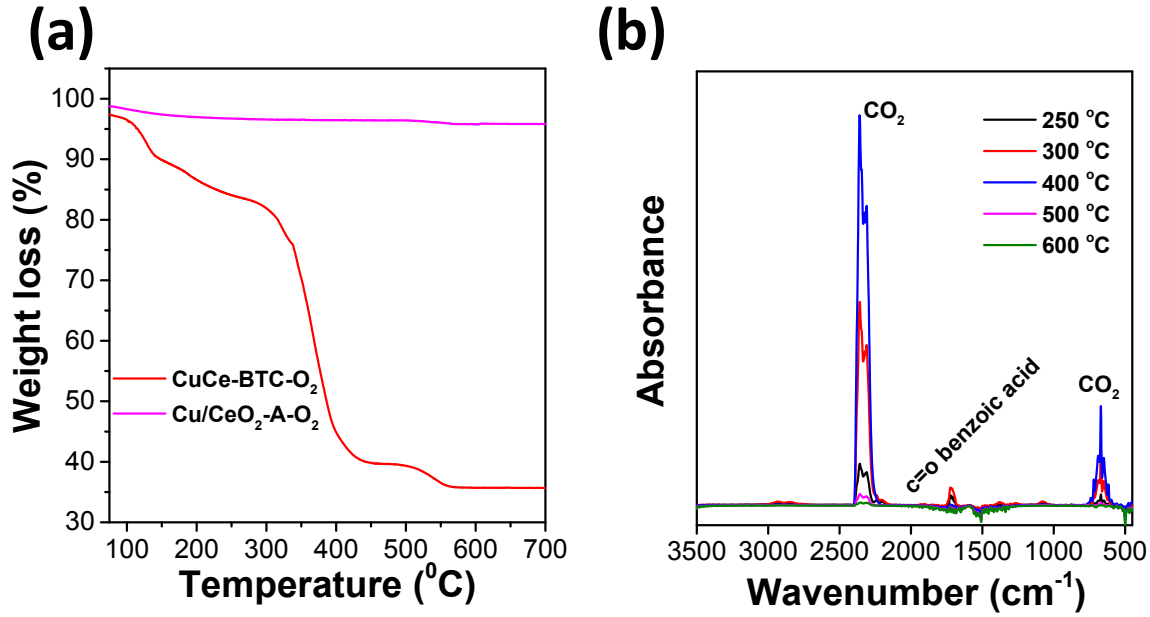

Fig. S1. (a,b)The coupled TGA-IR spectra of CuCe-BTC and Cu/CeO_2-A catalysts in the presence of O_2.

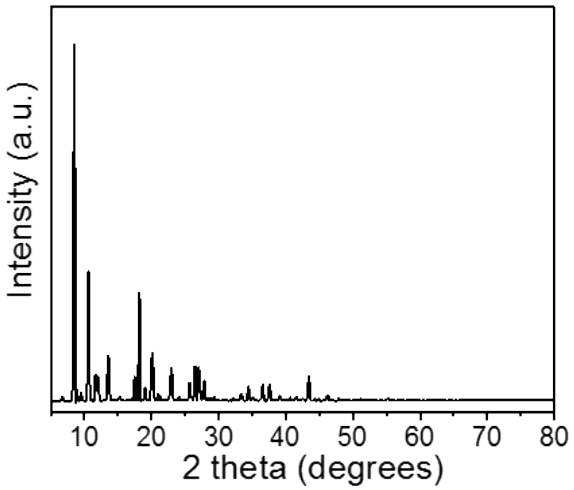

Fig. S2. Powder X-ray diffraction (XRD) pattern of CuCe-BTC catalyst.

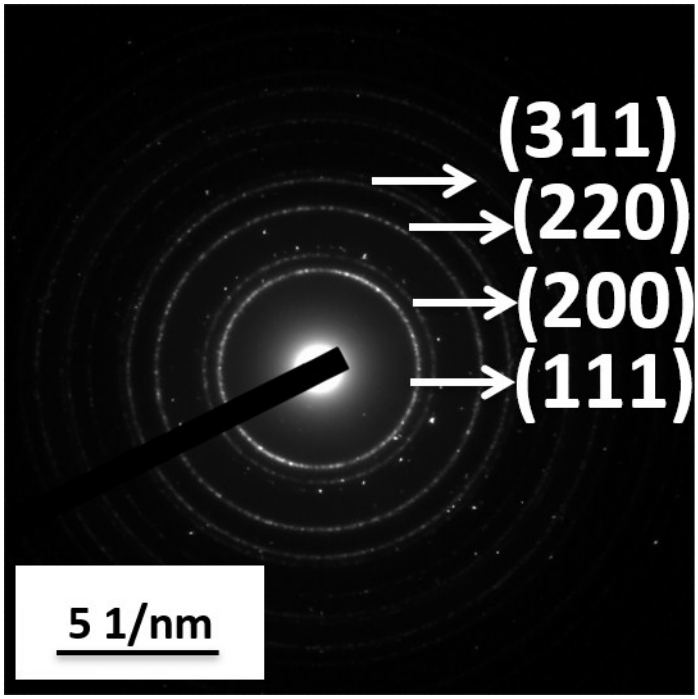

Fig. S3. Selected area electron diffraction (SAED) pattern of Cu/CeO_2-A catalyst.

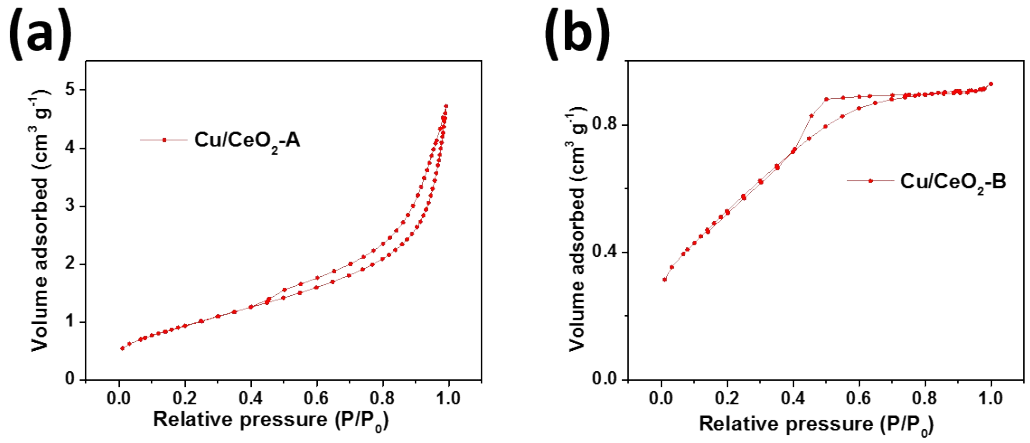

Fig. S4. N_2 sorption isotherms of (a) Cu/CeO_2-A and (b) Cu/CeO_2-B catalysts.

Table S1: N_2 BET surface areas, average pore volumes, crystallite size, Cu dispersion, and CuO loading values of Cu/CeO_2-A and Cu/CeO_2-B catalysts.

Catalyst	Surface area (m^2/g)[a]	Average pore volume (cm^3/g)[a]	CeO_2 crystallite size (nm)[b]	CuO crystallite size (nm)[b]	Cu crystallite size (nm)[c]	Cu dispersion (%)[c]	CuO loading (wt.%)[d]
Cu/CeO_2-A	103	0.11	6.85	7.4	6.2	4.2	9.87
Cu/CeO_2-B	61	0.03	10.39	9.8	10.2	2.6	9.80

[a]Determined from N_2 BET isotherms

[b]Determined from Scherrer equation

[c]Determined from N_2O chemisorption

[d]Determined from MP-AES analysis

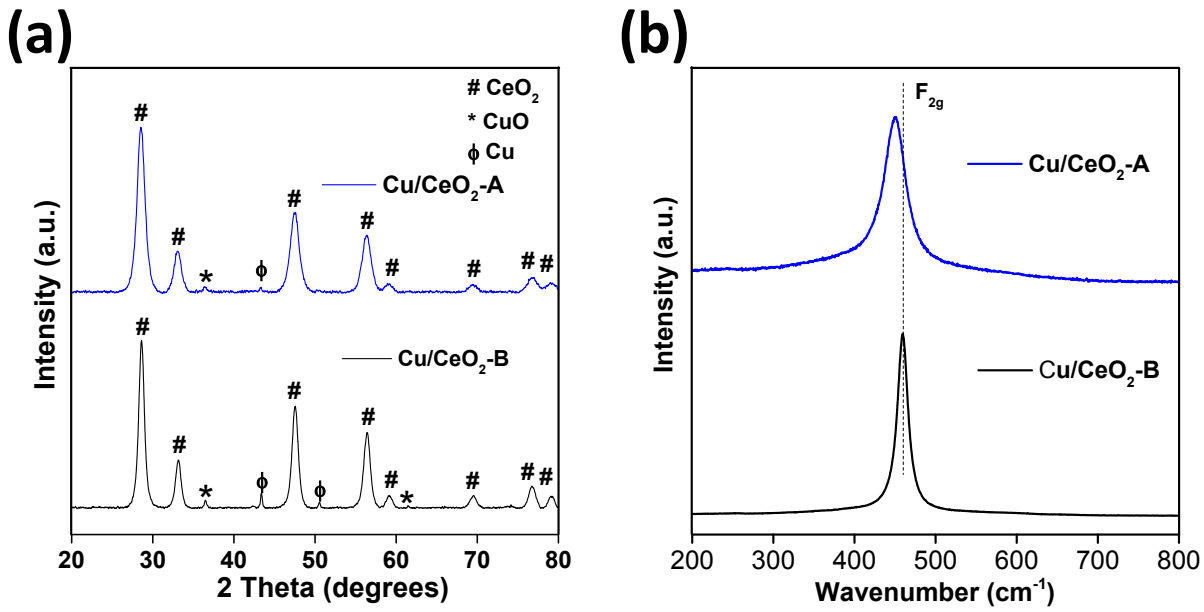

Fig. S5. (a) XRD and (b) Raman spectra of Cu/CeO_2-A and Cu/CeO_2-B catalysts.

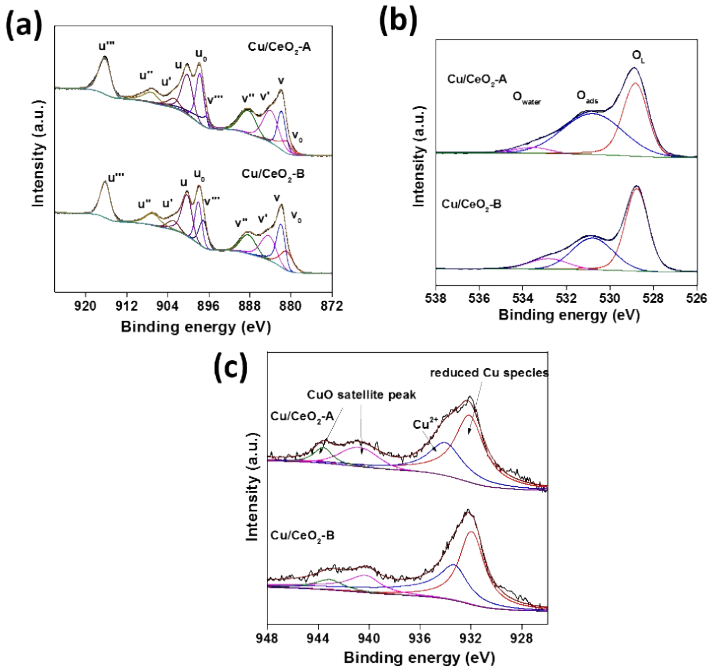

Fig. S6. (a) Ce 3d, (b) O 1s, and (c) Cu 2p XPS spectra of Cu/CeO_2-A and Cu/CeO_2-B catalysts.

Table S2. Surface atomic ratio determined by XPS**.**

Catalyst	Cu species (%)		Ce species (%)			O species (%)		
	CuO	Reduced Cu	Ce^{3+}	Ce^{4+}	Ce^{3+}/Ce^{4+}	O_L	O_{ads}	O_{water}
Cu/CeO_2-A	41.8	58.2	45.2	54.8	0.82	41.5	52.1	6.4
Cu/CeO_2-B	48.3	51.7	40.4	59.6	0.67	56.2	35.2	8.6

O_L=lattice oxygen; O_{ads}=surface adsorbed oxygen; O_{water}=oxygen associated with water

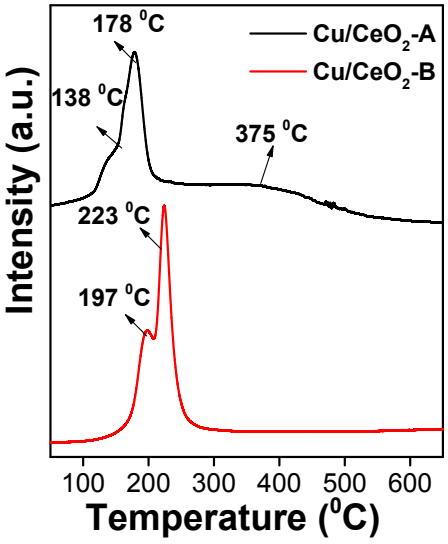

Fig. S7. H_2-TPR patterns of the Cu/CeO_2-A and Cu/CeO_2-B catalysts.

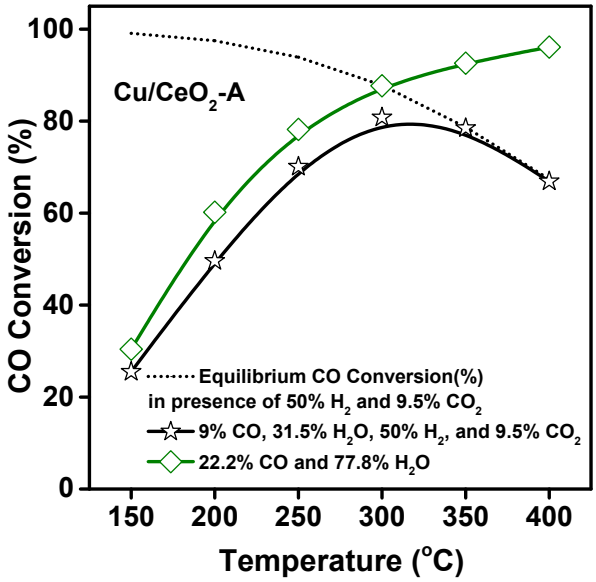

Fig. S8. Water-gas shift performance of Cu/CeO_2-A catalyst under realistic conditions.

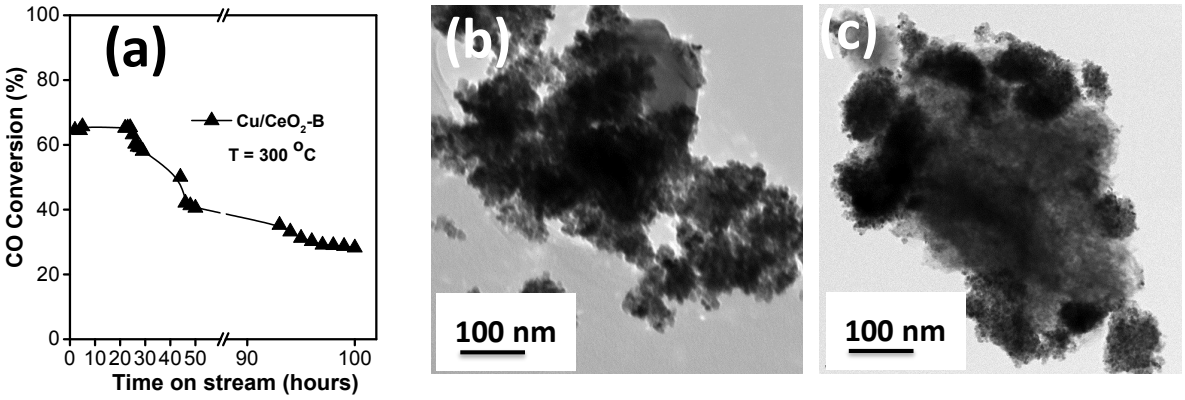

Fig. S9. (a) CO conversion as a function of time on stream for the Cu/CeO_2-B catalyst. TEM images of Cu/CeO2-B catalyst, (b) fresh and (c) spent.

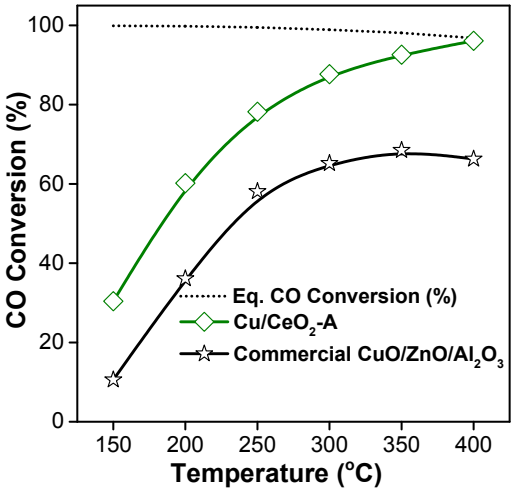

Fig. S10. Comparison of the water-gas shift activity of Cu/CeO_2-A catalyst with the commercial $CuO/ZnO/Al_2O_3$ catalyst.

Table S3: WGS activity comparison of MOF derived Cu/CeO_2 catalyst with the reported catalysts.

Catalyst	WGS reaction feed compositions	Temperature (°C)	Activation energy E_a (kJ/mol)	Reference
Cu/CeO_2-MOF	22.2% CO, 77.8% H_2O	180-260	35	The present study
8 wt.% CuO-CeO_2	7% CO, 22% H_2O, 8.5% CO_2, 37% H_2, balance Ar	240	56	1
4–10 at.% Cu–CeO_2	12.9% CO, 19.7% H_2O, 12.2% CO_2, 55.2% H_2	-	45–54	2
1.5–19.6 at.% Cu–CeO_2	2% CO, 10% H_2O, balance He	150-250	40–60	3
5%Cu/CeO_2 (Alfa Aesar)	5% CO, 10% H_2O, balance N_2	200-400	60	4
5%Cu/CeO_2 (Nanophase)	5% CO, 10% H_2O, balance N_2	200-400	60	4
5%Cu/CeO_2(combustion)	5% CO, 10% H_2O, balance N_2	200-400	44	4
40%CuO/ZnO/Al_2O_3	7% CO, 22% H_2O, 8.5% CO_2, 37% H_2, 25% Ar	190	79	1
42% CuO-ZnO-Al_2O_3 (G-66 A)	0.5 mol% CO and 1.5 mol% H_2O in He	123-175	47	5
CuO/ZnO/Al_2O_3	-	180-200	86	6

1. N.A. Koryabkina, A.A. Phatak, W.F. Ruettinger, R.J. Farrauto, F.H. Ribeiro, *J. Catal*. 2003, **217**, 233–239.
2. C. Zerva, C.J. Philippopoulos, *Appl. Catal. B* 2006, **67**, 105–112.
3. R. Si, J. Raitano, N. Yi, L. Zhang, S.-W. Chan, M. Flytzani-Stephanopoulos, *Catal. Today* 2012, **180**, 68–80.
4. P. Tepamatr, N. Laosiripojana, S. Charojrochkul, *Appl. Catal. A* 2016, **523**, 255–262.
5. H. Kušar, S. Hočevar, J. Levec, *Appl. Catal. B* 2006, **63**, 194–200.
6. C.V. Ovesen, B.S. Clausen, B.S. Hammershoei, G. Steffensen, T. Askgaard, I. Chorkendorff, J.K. Nørskov, P.B. Rasmussen, P. Stoltze, P. Taylor, *J. Catal.* 1996, **158**, 170–180.